Available online at www.sciencedirect.com
ScienceDirect
Journal of Pharmaceutical and Biomedical Analysis 43 (2007) 14–23
JOURNAL OF PHARMACEUTICAL AND BIOMEDICAL ANALYSIS
www.elsevier.com/locate/jpba

Hyphenation of Raman spectroscopy with gravimetric analysis to interrogate water–solid interactions in pharmaceutical systems

Alan D. Gift, Lynne S. Taylor*

Purdue University, Industrial and Physical Pharmacy, 575 Stadium Mall Dr., West Lafayette, IN 47907, United States

Received 7 April 2006; received in revised form 13 June 2006; accepted 15 June 2006
Available online 1 August 2006

Abstract

A moisture sorption gravimetric analyzer has been combined with a Raman spectrometer to better understand the various modes of water–solid interactions relevant to pharmaceutical systems. A commercial automated moisture sorption balance was modified to allow non-contact monitoring of the sample properties by interfacing a Raman probe with the sample holder. This hybrid instrument allows for gravimetric and spectroscopic changes to be monitored simultaneously. The utility of this instrument was demonstrated by investigating different types of water–solid interactions including stoichiometric and non-stoichiometric hydrate formation, deliquescence, amorphous–crystalline transformation, and capillary condensation. In each of the model systems, sulfaguanidine, cromolyn sodium, ranitidine HCl, amorphous sucrose and silica gel, spectroscopic changes were observed during the time course of the moisture sorption profile. Analysis of spectroscopic data provided information about the origin of the observed changes in moisture content as a function of relative humidity. Furthermore, multivariate data analysis techniques were employed as a means of processing the spectroscopic data. Principle components analysis was found to be useful to aid in data processing, handling and interpretation of the spectral changes that occurred during the time course of the moisture sorption profile.

Keywords: Raman spectroscopy; Moisture sorption; Multivariate data analysis; Water–solid interactions; Hydrate transformation; Amorphous; Crystallization; Deliquescence

1. Introduction

Understanding the response of pharmaceutical solids to external stresses such as temperature and relative humidity (RH) is a key part of drug development. It is well established that exposure to high relative humidity can promote chemical and physical instability. There are multiple mechanisms through which water can interact with solids as reviewed by Zografi [1,2]. The major mechanisms of pharmaceutical interest include adsorption to solid surfaces, absorption into the bulk of disordered structures, capillary condensation in porous materials, deliquescence, and anhydrate–hydrate phase transformations.

Due to the importance of water–solid interactions, moisture sorption profiles, which describe the relationship between water content and RH at a specific temperature, are normally procured for active pharmaceutical ingredients and pharmaceutical excipients. The current method of choice to determine water vapor sorption profiles is through gravimetric measurement whereby a small sample is placed on a sensitive analytical balance and subjected to a program of different RHs. Automated systems are commercially available and the generation of moisture sorption profiles has become a routine part of drug development.

The resultant moisture sorption profiles provides information about the water content of a sample as a function of RH and gravimetric analysis can be considered as a somewhat indirect technique as no chemical information is provided. Therefore, in some instances the mechanism of the water interaction with the solid and physical transformations within the solid can be ambiguous and require further investigation with other techniques. Interfacing another analytical technique to a moisture sorption balance (MSB) could thus be useful to enhance understanding of the influence of sorbed water on physical properties. Vibrational spectroscopy is an ideal technique for this purpose since it is non-invasive, non-destructive, and no sample preparation is required. In previous studies, Buckton showed that near infrared spectroscopy (NIR) could be interfaced with a MSB [3,4]. While NIR systems have shown considerable utility as monitoring techniques due to the relative ease of remote sam-

* Corresponding author. Tel.: +1 765 496 6614; fax: +1 765 494 6545.
E-mail address: ltaylor@pharmacy.purdue.edu (L.S. Taylor).

0731-7085/$ – see front matter © 2006 Elsevier B.V. All rights reserved.
doi:10.1016/j.jpba.2006.06.025

pling, NIR spectra can be hard to interpret, and large quantities of moisture associated with a sample can dominate the spectrum [5]. The use of Raman spectroscopy in combination with gravimetric moisture sorption measurements has not been explored to date despite the fact that Raman spectra typically have sharp peaks and high information content. Furthermore, Raman spectroscopy is well established for the analysis of pharmaceutical solids and numerous studies exist which detail the characterization of polymorphs, hydrates and amorphous samples with this technique [6–9].

In this study, we have explored for the first time, the use of a hybrid technique combining Raman spectroscopy with a MSB. In order to evaluate the utility of this approach, several types of water–solid interaction were interrogated including stoichiometric hydrate formation, amorphous–crystalline transformation, deliquescence, non-stoichiometric hydrate formation, and capillary condensation. In addition, multivariate data analysis methods were explored as a means of processing the spectroscopic data.

2. Experimental

2.1. Materials

Crystalline sucrose was obtained from Mallinckrodt Baker Inc. (Phillipsburg, NJ). Sulfaguanidine monohydrate was obtained from Sigma–Aldich Inc. (St. Louis, MO) and sulfaguanidine anhydrous was formed by dehydrating sulfaguanidine monohydrate in an oven at 110 °C for 12 h. Ranitidine HCl and cromolyn sodium were obtained from Hawkins Inc. (Minneapolis, MN). Silica gel with a particle size of 40–63 μm, a pore diameter of 60 Å and a specific surface area of 500 m^2/g was obtained from Silicycle (Quebec, QC, Canada).

Amorphous sucrose was prepared by lyophilizing an aqueous sucrose solution (15 g per 100 ml) using a Lyostar freeze-drier (FTS Systems, Stone Ridge, NY). The freeze drying program for the sucrose solution had a freezing step at −45 °C for 12 h. This was followed by applying a vacuum for primary drying using a shelf temperature of −15 °C for 24 h and a secondary drying step at +15 °C for 24 h. A well-formed cake resulted and X-ray powder diffraction confirmed the lyophilized sucrose was amorphous.

2.2. Methods

The moisture sorption profiles for the model compounds were generated using a symmetric gravimetric analyzer (SGA-100, VTI Corporation, Hialeah, FL). A schematic of this instrument is shown in Fig. 1. Samples ranging in mass from 2 to 15 mg were placed on the sample holder. The samples were dried in the SGA-100 at 50 °C for a maximum of 180 min to remove any residual moisture. The sorption profiles were collected at 25 °C as the samples were exposed to increasing levels of relative humidity (RH). The equilibrium criterion for each RH step was 0.001% w/w in 5 min with a maximum step time of 180 min.

Raman spectra of the samples were collected using a RamanRxn1-785 Raman spectrometer (Kaiser Optical Systems, Inc., Ann Arbor, MI) with a laser wavelength of 785 nm. The spectra were obtained using a fiber-optic MR probe (Kaiser Optical Systems, Inc., Ann Arbor, MI) equipped with a 10× microscope objective (Olympus, Japan) with a working distance of approximately 7 mm which focused the laser light onto the sample. Spectra were collected every 2 min and each spectrum was the average of 8 spectra, each with an integration time of 13 s. The laser power at the sample was measured to be about 150 mW using a Coherent LaserCheck power meter (Auburn, CA).

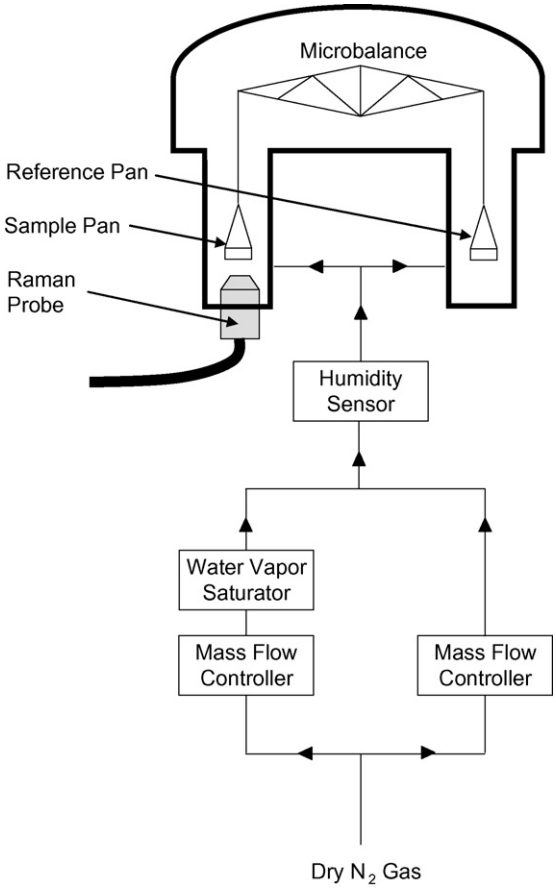

Fig. 1. Schematic representation of the combined Raman-moisture sorption balance (Raman-MSB) instrument.

The SGA-100 was modified by the manufacturer for the addition of a Raman probe in the sample compartment. An aperture was constructed below the sample chamber to produce an air-tight seal with the microscope objective which was attached to the MR probe which in turn was fiber-optically coupled to the spectrometer. The sample pan had a glass disc as its bottom so the sample can be illuminated by the Raman probe from below as shown in Fig. 1. If needed, the glass disc can be removed and replaced with other transparent materials such as quartz or sapphire.

2.3. Software

Flow System II Software (Version 2.02.01, VTI Corporation, Hialeah, FL, USA) was used to collect the moisture sorption profiles on the gravimetric analyzer. HoloGRAMS Software

(Version 4.0, Kaiser Optical Systems, Inc., Ann Arbor, MI) was used to control the Raman spectrometer. Excel 2003 (Microsoft Corporation, Seattle, WA) was used for analysis of SGA sorption profiles, calibration calculations and graph plotting. SIMCA-P+ (Version 10.5, Umetrics AB, Umeå, Sweden) was used for principle components analysis.

2.4. Principal component analysis

Principal component analysis (PCA) was performed with SIMCA-P+ Software (Version 10.5, Umetrics AB, Umeå, Sweden) to aid in the analysis of the Raman spectroscopic data. PCA is a mathematical transformation method which projects spectra as points in a space with a small number of principal components (PCs). The PCs are extracted from the data in such a way that each PC explains as much of the observed spectral variation as possible. Each PC consists of two vectors, a score vector and a loading vector. The score vector contains a score value for each spectrum, which tells how the spectrum is related to the other spectra in that particular PC. The loading vectors show spectral features, where high absolute values indicate a large influence on the PCA model [10].

PCA was performed on spectral regions of the Raman spectra where peak heights changed or shifted during the time course of the moisture sorption profile. This range depended on the specific sample. All spectral data were mean centered before PCA was performed. Different processing methods were tested but only standard normal variate (SNV) transformed [11] or non-preprocessed data were used in the final PCA models.

3. Results and discussion

3.1. Sulfaguanidine

Sulfaguanidine (SGN) is an active pharmaceutical ingredient (API) that is capable of existing as both the anhydrate and monohydrate forms in the solid state. Sulfaguanidine monohydrate is a channel hydrate and the rate of interconversion between the hydrate and anhydrate is dependent on environmental RH. The Raman spectra of the anhydrate and the monohydrate have distinct differences in peak intensities and positions (Fig. 2). These differences can be used to differentiate and quantify the amounts of each crystalline form.

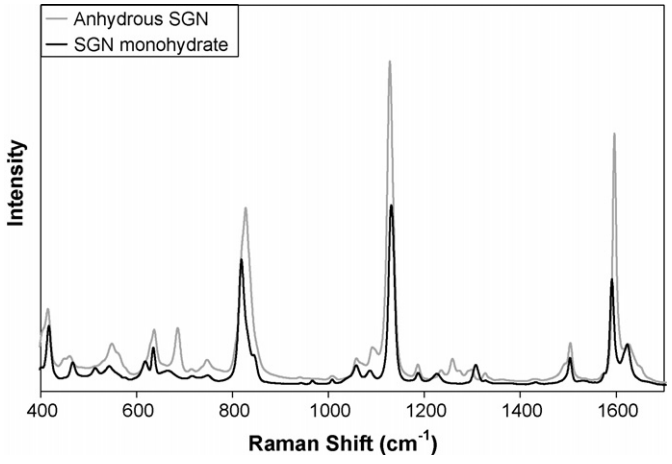

Fig. 2. Raman spectra of anhydrous sulfaguanidine (gray) and sulfaguanidine monohydrate (black).

The time course for the moisture sorption profile of SGN (Fig. 3a) showed that the sample did not begin to increase in weight until the relative humidity was increased to 65% RH. The increase in weight at 65% RH suggested that the sample was starting to transform to the hydrate. When the relative humidity was further raised to 75%, the slope of the weight gain profile became steeper, indicating an increase in the rate of anhydrate to hydrate transformation of the sulfaguanidine. The total weight percent change for the initially anhydrous sulfaguanidine was 8.1% which is close to the theoretical 8.4% increase that would be expected on monohydrate formation.

The Raman spectra collected during the moisture sorption experiment confirmed the transformation of SGN anhydrate to SGN monohydrate as the RH was increased. The spectra collected at the beginning and end of the run corresponded well with the spectra in Fig. 2 representing the anhydrate and hydrate forms of SGN. Furthermore, between 700 and 900 min of the

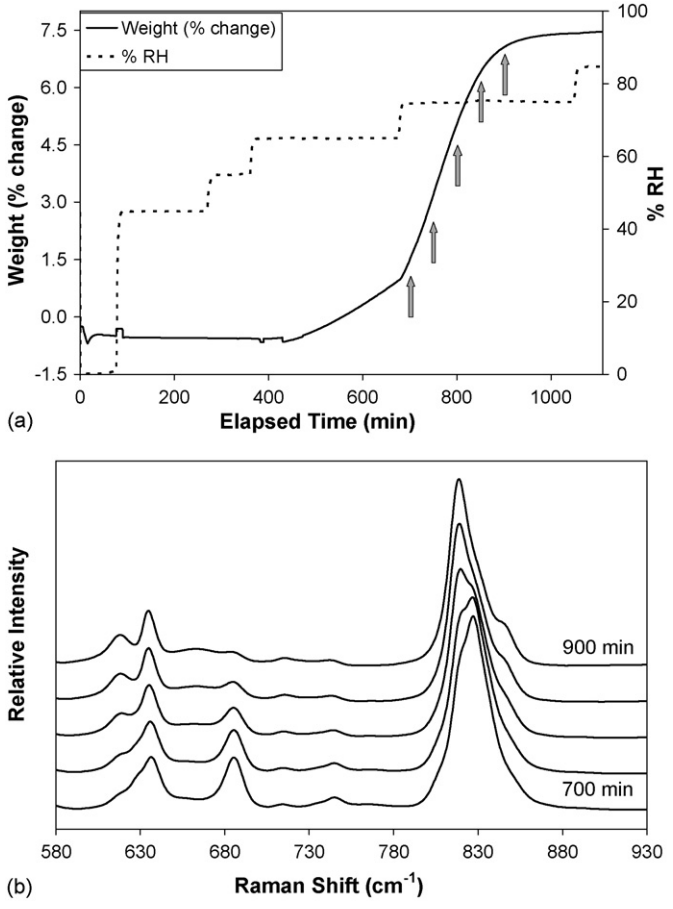

Fig. 3. (a) Moisture sorption profile of anhydrous sulfaguanidine (sample size of 9.717 mg). The dashed line represents the relative humidity in the sample chamber and the black line represents the percent change in weight of the sulfaguanidine sample as the humidity is increased. Arrows indicate time points of spectra shown in (b). (b) Raman spectra of sulfaguanidine collected during the moisture sorption profile. The spectra displayed were collected between 700 and 900 min at 50 min intervals.

moisture sorption profile, changes in the SGN Raman spectrum became evident as shown by the spectra in Fig. 3b. These changes included the disappearance of a peak at 685 cm^{-1}, the shift in peak from 828 to 819 cm^{-1}, and the rise in a shoulder peak at 617 cm^{-1}. The time frame for these spectral changes was in good agreement with the rise in mass of the sample in the moisture sorption profile (Fig. 3a).

The spectral data were used to quantitate the percent conversion of the SGN yielding a spectral transformation profile. To achieve this, a calibration curve was constructed by collecting Raman spectra of known ratios of powder blends of anhydrous and monohydrate sulfaguanidine. A bivariate calibration model for overlapping peaks was used to determine the ratio of anhydrate to hydrate material from the peak heights [8]. For this calibration the 828 cm^{-1} peak for anhydrous sulfaguanidine and the 819 cm^{-1} peak for sulfaguanidine monohydrate were used. The calibration curve had good linearity with an R^2 of 0.986 and root mean square error of calibration of 5.2%. The amount of SGN hydrate was then determined at each time point during the moisture sorption experiment and the spectral transformation profile was generated. As seen from Fig. 4a, in general, close agreement was observed between the spectral transformation profile (black line) and the percent weight change of the sample (gray line). A discrepancy was observed at the beginning of the transformation where the moisture sorption profile indicated that moisture uptake began at about minute 400, whereas the spectral transformation profile suggested that hydrate transformation began at about minute 700. The most probable explanation for this discrepancy was due to the sample thickness and the positioning of the Raman probe. The SGN hydrate transformation started to occur at the top of the sample because it has the most contact with the humid atmosphere but the Raman spectra were collected from the bottom of the sample (Fig. 1) thus there was a delay time as the moisture diffuses through the SGN sample.

For SGN, it was possible to construct a transformation profile using a calibration curve but in many instances this is either not possible or too time consuming, hence it is of interest to explore other analysis methods that can be used to extract information from the spectra. In these situations, multivariate data analysis, such as principal components analysis (PCA) can be a useful approach to interpret Raman spectral changes occurring during the time course of the moisture sorption experiment.

A PCA was performed on the Raman spectra collected during the moisture sorption profile. The selected spectral range was from 350 to 1650 cm^{-1} and the data were preprocessed using the SNV transform and mean centered prior to analysis. The first principal component captured 99.7% of the variation. The weighted scores for the first principal component are shown in Fig. 4a. The scores for this PCA model indicated the SGN spectrum began to change at about 700 min and this spectral change leveled off at about 1000 min. Scores for this first PC corresponded closely with the transformation profile calculated with the bivariate calibration. This was expected since the spectral change represented by the scores encompasses the same variation captured by the bivariate calibration model. It should be noted that the PCA model was not a quantitative method and only appears quantitative in Fig. 5 because the data were scaled to match the bivariate transformation profile. However, the scores are useful for displaying the trends in spectral changes as a function of exposure to moisture. Furthermore, by interpreting the loadings, the underlying basis for the change in score values can be interpreted. In Fig. 4b, the loadings for the first PC are

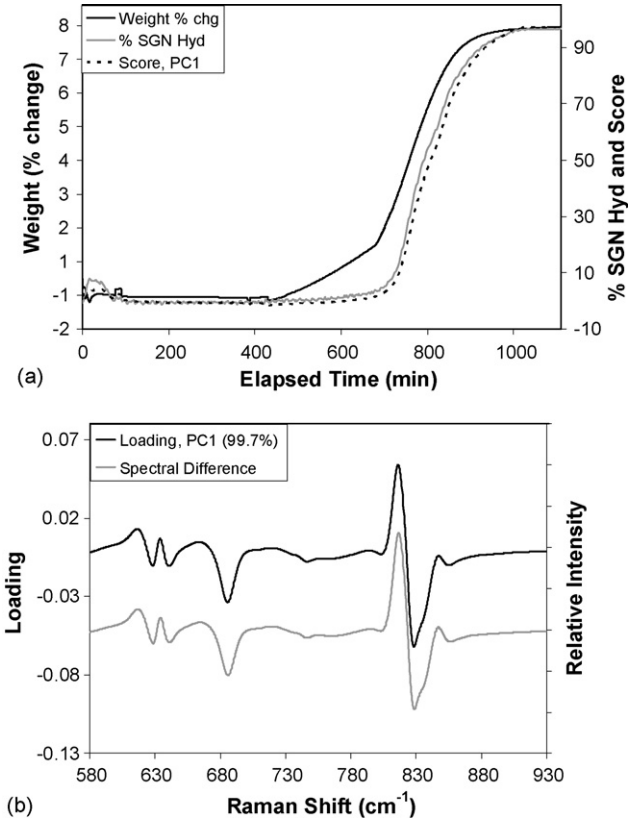

Fig. 4. (a) Spectral transformation profile, moisture sorption profile, and scores of sulfaguanidine. The black line represents the amount (percent) of sulfaguanidine monohydrate present in the sample determined by spectral data. The gray line represents the percent change in weight of the sulfaguanidine sample and the dashed line represents the scores of the first principal component of the PCA. (b) Loadings of the first principal component compared to the weighted spectral difference of anhydrate and hydrate sulfaguanidine.

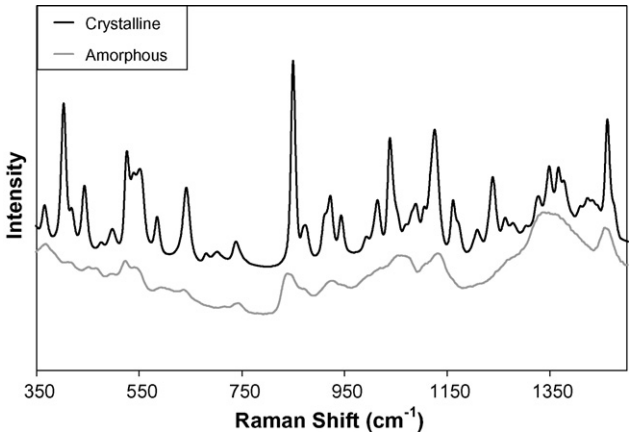

Fig. 5. Raman spectra of crystalline sucrose (black) and amorphous sucrose (gray).

compared to the spectral difference of anhydrate and hydrate SGN. The spectral difference, obtained by subtracting the anhydrate spectrum from the hydrate spectrum, was very similar to the loading vector. This comparison demonstrates that the variation modeled using the chemometric method arises from the conversion of SGN anhydrate to the hydrate form and that the score values are a useful method for qualitative monitoring of the progress of the conversion.

3.2. Amorphous sucrose

Sucrose is commonly used as an excipient in pharmaceutical systems and thus there has been extensive research into its properties both in the amorphous and crystalline state. The metastable amorphous state has a higher molecular mobility relative to the stable crystalline phase. When the amorphous material absorbs water, molecular mobility is increased and crystallization will occur reducing the energy of the system [12]. Differences between the amorphous and crystalline form of a compound can generally be detected using Raman spectroscopy [8]. Crystalline materials tend to have sharp intense peaks when compared to the broad peaks present in the amorphous form. This is evident in Fig. 5 which shows the Raman spectra of crystalline and amorphous sucrose.

Crystalline sucrose was rendered amorphous by lyophilization as detailed in the experimental section. The time course for the moisture sorption profile of amorphous sucrose (Fig. 6a) showed that at each successive RH step up to 60% the mass of the amorphous sucrose sample increased. The increase in mass was halted when the relative humidity was raised to 60%. At that point the mass of the sample began to decrease. This decrease in mass continued until the sample reached close to the original mass. The decrease in weight was consistent with crystallization of the sample [13].

The Raman spectra confirmed the amorphous to crystalline transformation of sucrose. Fig. 6b shows Raman spectra collected at four different time points (300, 400, 500, and 600 min) during the moisture sorption profile. As the humidity was raised the sucrose sample increased in mass due to the absorption of water. This water absorption had little effect on the Raman spectrum as shown by the amorphous character of the spectra collected at 300 and 400 min (compare to the pure amorphous spectrum in Fig. 5). When the sucrose started to lose mass at about 430 min, crystallization of the amorphous material had begun [13]. Since crystalline sucrose is anhydrous, crystallization leads to expulsion of moisture and the observed decrease in mass [13]. The presence of crystalline material can be clearly observed in the Raman spectra obtained at 500 and 600 min (Fig. 6b).

Further spectral analysis was performed using PCA with SNV preprocessing. Spectra obtained during the decrease in mass of the sucrose sample that occurred between 400 and 680 min were analyzed. The resultant model had one relevant PC that contained 95.8% of the spectral variation. Interpretation of this PC supported the conclusion that the amorphous sucrose crystallized during this time period. The scores for this first PC (Fig. 7a) showed that there are significant spectral changes that

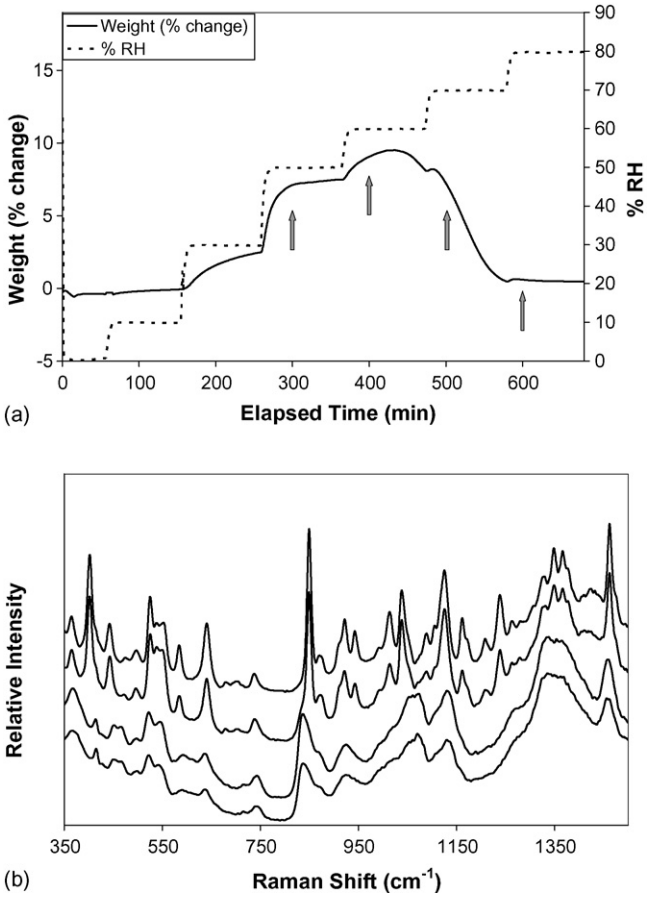

Fig. 6. (a) Moisture sorption profile of amorphous sucrose (sample size of 8.609 mg). The dashed line represents the relative humidity in the sample chamber and the black line represents the percent change in weight of the sulfaguanidine sample as the humidity is increased. Arrows indicate time points of spectra shown in (b). (b) Raman spectra of sucrose collected during the moisture sorption profile. Spectra from bottom to top were collected at times 300, 400, 500, and 600 min, respectively. Spectra were background subtracted to remove signal from sample pan.

occurred between 475 and 550 min of the moisture sorption profile and these changes corresponded well with the decrease in mass of the sample (Fig. 6a). In addition, a comparison of the loading vector for this PC with the weighted spectral difference between amorphous and crystalline sucrose (Fig. 7b) confirmed that the scores represented the increasing crystalline character of the spectra. It is also interesting to note that the score values indicated that the spectra started to change from amorphous to crystalline at 475 min even though the moisture sorption profile started to lose mass at 450 min. This delay is most likely due to the thickness of the sample and that crystallization began at the top surface of the sample. Thus several minutes probably elapsed before crystallization occurred in the bottom layer of the sample and was detected by the spectrometer. Furthermore, based on the score values, crystallization was complete at 550 min although there was still a loss of sample mass until 585 min. A reasonable explanation for the discrepancy in times between the termination of the crystallization and the loss of mass had to do with the kinetics of evaporation. Even though crystallization finished at 550 min it appears to

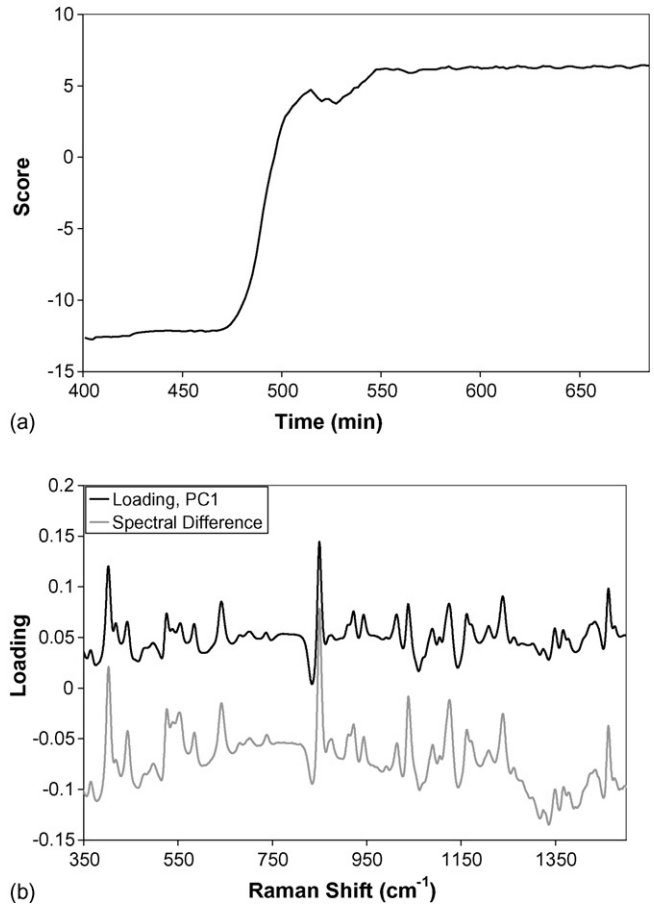

Fig. 7. PCA of crystallization of amorphous sucrose. (a) Scores of the PC showing spectral variation beginning at 475 min and ending at 550 min. (b) Loadings of the PC compared to spectral difference between amorphous and crystalline sucrose.

have taken an additional 35 min before all the water evaporated at 70% RH.

3.3. Ranitidine HCl

Ranitidine HCl, a widely used H_2 receptor antagonist used to control stomach acidity, can interact with water through the phenomenon of deliquescence [14,15]. Deliquescence is a phase transformation whereby a substance absorbs water vapor from the atmosphere, leading to the dissolution of the solid [2]. The RH where deliquescence occurs is a characteristic of the solid at a particular temperature and this RH is termed the deliquescence point or critical relative humidity (RH_0). The RH_0 for ranitidine HCl has previously been determined to be 76% RH at 25 °C [14,15]. Below RH_0, minimal amounts of water will adsorb to the ranitidine crystalline surface whereas above RH_0, crystalline ranitidine begins to dissolve in the condensate film collecting on the surface. Raman spectra were collected for both crystalline and aqueous ranitidine HCl to determine the spectral contrast between the two phases. These spectra (Fig. 8) show the broader peaks that are associated with the aqueous phase when compared to the crystalline phase. This peak broadening is most notable in the 1150–1650 cm^{-1} region of the spectrum.

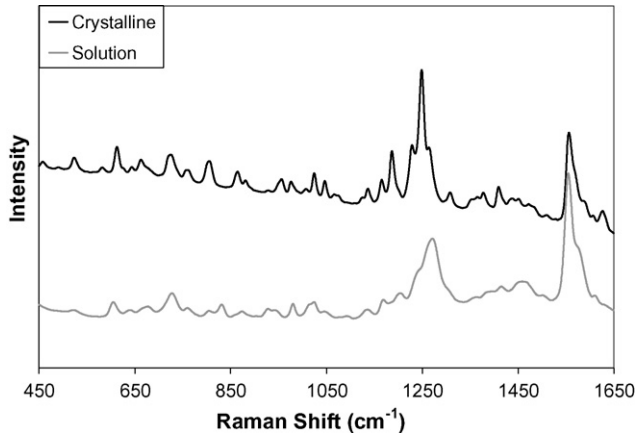

Fig. 8. Raman spectra of crystalline ranitidine HCl (black) and an aqueous solution of ranitidine HCl (gray).

The time course for the moisture sorption profile of ranitidine HCl (Fig. 9a) shows that at low relative humidities (0–60%) the sample mass did not change significantly. As the relative humidity approached 76%, the mass of the ranitidine HCl began to

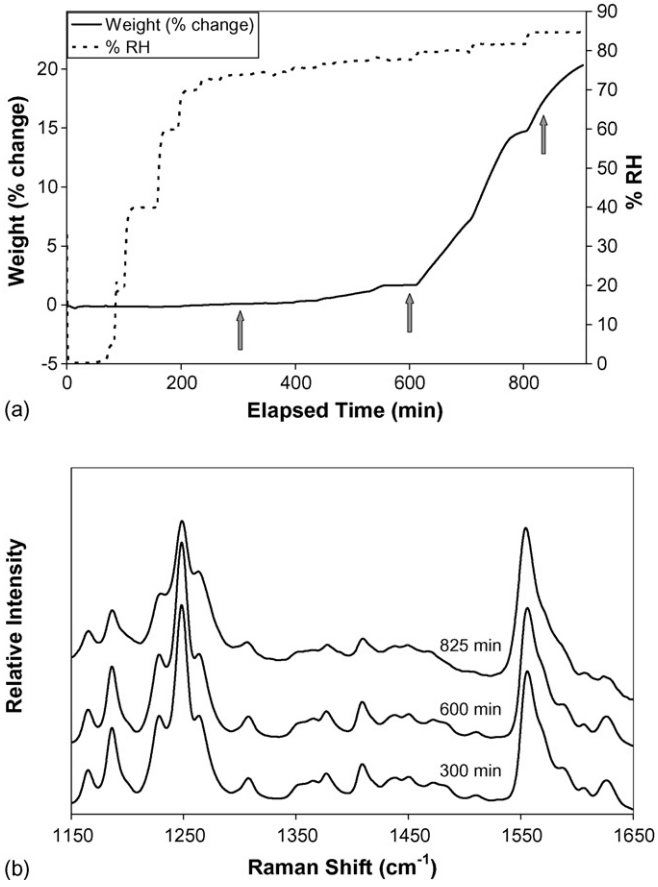

Fig. 9. (a) Moisture sorption profile of ranitidine HCl (sample size of 14.115 mg). The dashed line represents the relative humidity in the sample chamber and the black line represents the percent change in weight of the sulfaguanidine sample as the humidity is increased. Arrows indicate time points of spectra shown in (b). (b) SNV transformed Raman spectra collected during the moisture sorption profile of ranitidine HCl. Spectra from bottom to top were collected at times 300, 600 and 825 min.

slowly increase. However, when the RH was raised above 76%, the sample mass increased rapidly. These data are consistent for a deliquescence compound with a critical RH_0 of 76%.

The Raman spectra collected during the moisture sorption profile helped to confirm the deliquescence of ranitidine. Raman spectra at three different time points are shown in Fig. 9b. No change in spectral shape was observed between 300 and 600 min, however, modest spectral changes were observed between 600 and 825 min. The most obvious change was the broadening of the three peaks centered at 1248 cm^{-1}. This broadening of peaks was in agreement with a deliquescent material where a portion of the sample enters the solution phase. Although the spectrum at 825 min was not identical to the aqueous ranitidine HCl spectrum (Fig. 8), it did appear to be gaining more aqueous character. This change from crystalline to aqueous character was expected because as the ranitidine HCl deliquesced, a higher proportion of the crystalline ranitidine would have dissolved into the sorbed water until eventually the entire sample would be in solution. Based on the known solubility of ranitidine HCl (3.2 g ranitidine/g H_2O) [16] and the total mass of water gained by the sample, it would be expected that a significant fraction of the material would still be crystalline, which explains why the Raman spectra in Fig. 9b still show crystalline character.

A PCA was performed on spectra collected between 400 and 900 min to further explore the deliquescence of ranitidine HCl. Spectra were preprocessed using SNV transformation and mean centered prior to analysis. The PCA model returned one significant principal component which contained 95.9% of the spectral variation. The scores for this PC (Fig. 10a) indicated the spectral change began at about 760 min and ended at about 830 min. The loading vector for this PC is shown in Fig. 10b along with the spectral difference of aqueous and crystalline ranitidine HCl. The close similarity between the loading vector and the spectral difference confirmed that the spectral change corresponded to ranitidine HCl transforming from a crystalline state to an aqueous state.

The scores in Fig. 10a indicated that the spectral change began at about 760 min even though deliquescence began at about 450 min as shown by the moisture sorption profile in Fig. 9a. The reason for this delayed effect in the spectrum again had to do with sample thickness. Just as with the transformation of sulfaguanidine, the deliquescence of ranitidine HCl began at the top of the sample and there was a delay before the deliquescence was observed by the Raman probe at the bottom of the sample.

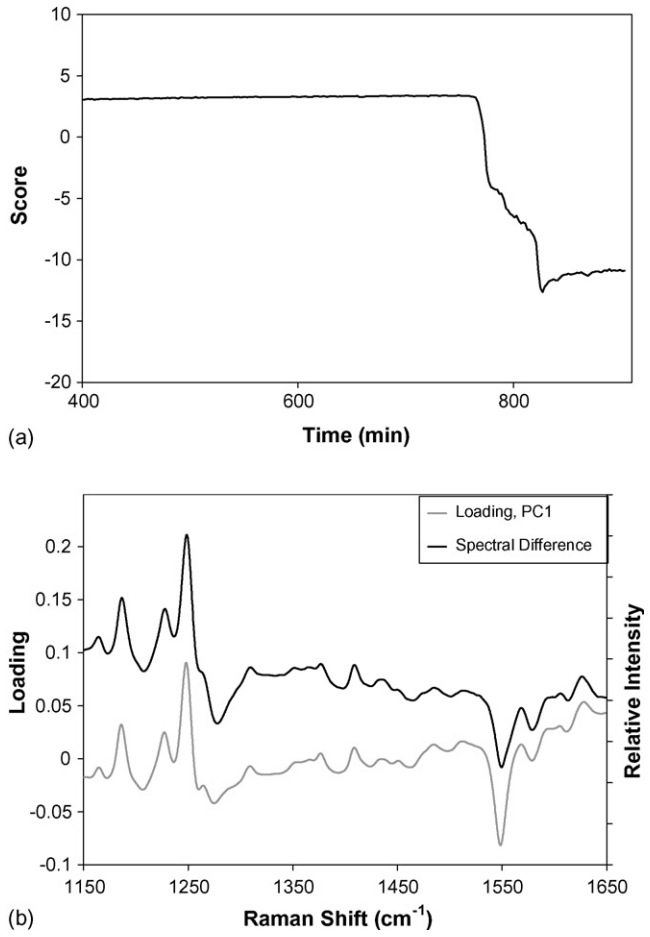

Fig. 10. PCA of crystallization of deliquescence of ranitine HCl. (a) Scores of the PC showing spectral variation beginning at 400 min and ending at 903 min. (b) Loadings of the PC compared to the Raman spectral difference between crystalline and aqueous ranitindine HCl.

3.4. Cromolyn sodium

Cromolyn sodium (CS), also known as disodium cromoglycate, is known to form a non-stoichiometric crystalline hydrate. CS is able to sorb and liberate water continuously and reversibly as a function of RH to give an infinite series of nonstoichiometric hydrates [17,18]. As the storage RH is increased, the CS crystal structure is able to expand the unit cell to accommodate up to nine molecules of water before collapsing to form a liquid crystalline state [17,18]. This unit cell expansion is accompanied by modest changes in the crystal structure such as differences in the torsional angles of the two carboxylate groups and the torsional and bond angles of the 2-hydroxypropane linking chain [18]. Furthermore, it has been shown that the water molecules are necessary for holding the CS crystal structure together and that the crystallinity decreases gradually as the RH is decreased beyond a critical point [18]. These changes in the crystal structure are observable in the Raman spectrum through peak shifts and peak intensity changes, especially in the carbonyl stretching region.

Prior to running the moisture sorption profile, the CS was stored at 0% RH (P_2O_5) in a desiccator for 1 week. The time course for the moisture sorption profile of CS (Fig. 11) showed that at each successive relative humidity step, the mass of the CS sample increased. Additionally, the step from 70 to 80% RH showed a disproportionately large jump in mass when compared to other 10% step increments in RH.

The Raman spectra collected during the experiment were analyzed using PCA. The spectra were pre-processed using a SNV transform and mean centered prior to analysis. The spectral region with the greatest variation, between 1150 and 1700 cm^{-1}, was used for data modeling. By examination of the data using various PCA models it was determined that there were two types of spectral variations occurring during the time course of the

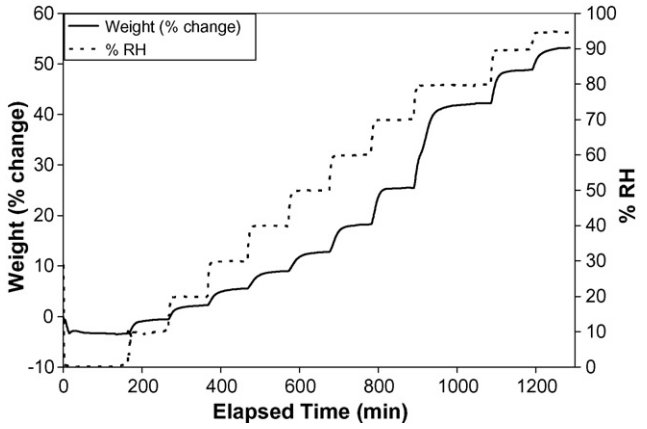

Fig. 11. Moisture sorption profile for cromolyn sodium (sample size of 2.094 mg). The dashed line represents the relative humidity in the sample chamber and the black line represents the percent change in weight of the sulfaguanidine sample as the humidity is increased.

moisture sorption experiment. The division between these two different spectral variations was the transition between 70 and 80% RH which occurs at about 890 min. Two different PCA models were developed for the two different spectral variations. This separation of the data into two different parts will aid in the spectral interpretation of the collected data [5].

The first PCA model was applied to spectral data collected between 165 and 890 min. This model had one significant principal component which contained 81.6% of the spectral variation. The loadings for this PC along with the SNV transformed spectra from the beginning and end of this time period are shown in Fig. 12a. The loading vectors indicated that subtle spectral changes occurred during this time period. For instance, the dip in the loading values around 1633 cm^{-1} reflected the sharpening of the carbonyl peak at 1650 cm^{-1} which resulted from the decrease in intensity of the shoulder peak at 1633 cm^{-1}. In addition, the peak in the loading vector at 1573 cm^{-1} reflected an increase in the intensity of this peak with time. Such spectral changes were likely caused by a change in crystallinity of the CS sample. The CS was stored at 0% RH for 1 week prior to analysis and in that time the crystallinity of the sample would be expected to have decreased [18]. As the RH was increased during the experiment, the crystallinity of CS would have increased [18], giving rise to sharper and more intense peaks.

The second PCA model was developed from spectral data collected between 885 and 1285 min. This model had one significant principal component which contained 91.9% of the spectral variation. The scores for these loadings (data not shown) indicated that most of the spectral variation occurred between 895 and 980 min. This time period corresponded to the large jump in mass of the CS sample that occurred when the RH was increased from 70 to 80% (see Fig. 11). Fig. 12b shows the loadings for this PC along with the SNV transformed spectra from the beginning and end of this second time period. The most notable change in the spectrum was the peak shift and intensity change of the carbonyl stretching region. As the RH was increased to 80%, the peak at 1651 cm^{-1} shifted 9 wavenumbers to 1660 cm^{-1}. This spectral change is represented by the large peak in the loading

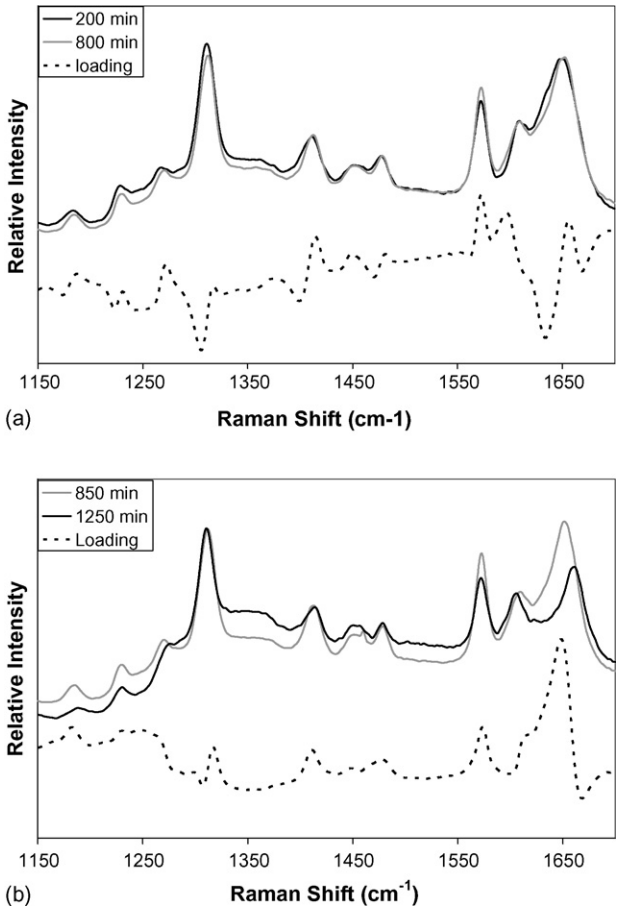

Fig. 12. (a) SNV transformed Raman spectra of cromolyn sodium collected at 200 and 800 min, and the loadings for the first principal component of the spectra collected between 165 and 890 min during the moisture sorption profile. (b) SNV transformed Raman spectra of cromolyn sodium collected at 850 and 1250 min, and the loadings for the first principal component of the spectra collected between 885 and 1285 min during the moisture sorption profile.

vector at 1650 cm^{-1}. These spectral changes were most likely due to unit cell expansion as more water molecules were incorporated into the crystal structure. Upon unit cell expansion, the CS crystal structure had increased flexibility and was able to rotate the two carboxylate groups away from each other [18]. The dramatic increase in water uptake above 70% RH would have caused this unit cell expansion and change in molecular confirmation which in turn would have resulted in the observed spectral changes in the carbonyl stretching region of the Raman spectra.

3.5. Silica gel

Silica gel is a porous form of silica (SiO_2) with a vast network of interconnected pores. These pores give silica gel a large surface area which will attract and hold water by adsorption and capillary condensation. Capillary condensation is said to occur when multilayer adsorption from a vapor proceeds to the point at which pore spaces are filled with liquid.

The time course for the moisture sorption profile of silica gel (Fig. 13a) showed that for each incremental step in relative

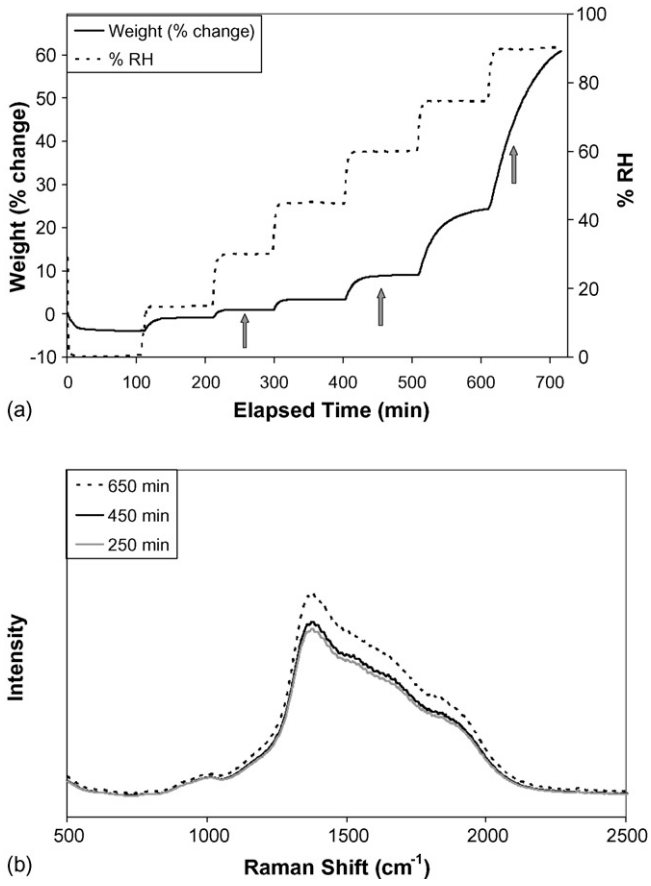

Fig. 13. (a) Moisture Sorption profile for silica gel (sample size of 7.396 mg). The dashed line represents the relative humidity in the sample chamber and the black line represents the percent change in weight of the sulfaguanidine sample as the humidity is increased. Arrows indicate time points of spectra shown in (b). (b) Raman spectra of silica gel collected during the moisture sorption profile of silica gel. Spectra from bottom to top were collected at time 250, 450, and 650 min, respectively.

humidity the mass of the sample increased and plateaued at a specific weight. This was as expected since the amount of water incorporated into the silica gel is dependent on the RH. As the RH increases, more water can be absorbed through capillary condensation.

The Raman spectrum of silica gel does not have any sharp distinct peaks but instead is composed of a broad spectral feature from 1000 to 2000 cm^{-1}. This broad feature is evident in Fig. 13b which shows spectra collected at times 250, 450, and 650 min during the moisture sorption profile. Upon visual inspection, it was difficult to see any changes in relative peak heights or peak shifts to the Raman spectra during the time course of the moisture sorption profile. The only changes evident were overall spectral intensity differences that evolved with time as shown in Fig. 13b.

A PCA was performed on the Raman data to determine if there were changes to the spectra as the silica gel absorbed water which were undetectable through visual inspection. This PCA model was mean centered without SNV transformation. The model returned only one significant principal component which contained 97.4% of the spectral variation. The scores for this first PC are shown in Fig. 14 along with the percent weight change of the moisture sorption profile. When comparing the two curves in Fig. 14 it is evident that the scores of the first PC track the weight change of the silica gel extremely well. The observed spectral variation was likely due the movement of the sample pan as the silica gel increased in weight. In other words, as silica gel absorbed water through capillary condensation, the sample pan was lowered closer to the Raman laser giving a higher Raman signal. Furthermore, the PCA model did not detect any changes in spectral shape such as the appearance or disappearance of peaks. This confirmed that no change in state of the silica gel occurred during the moisture sorption profile as expected for the absorption of water through capillary condensation.

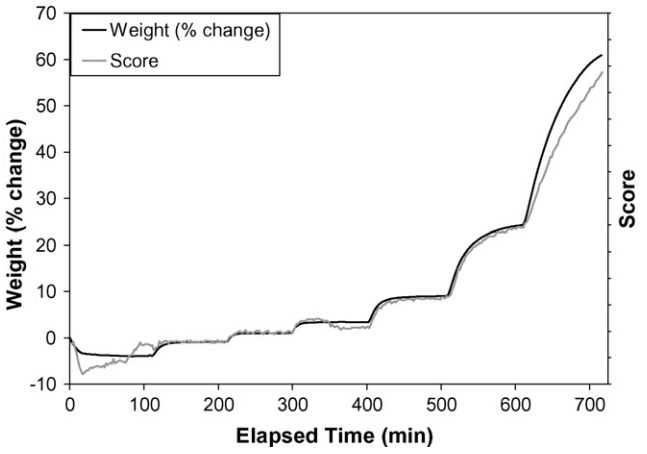

Fig. 14. Scores of the first principal component compared to the moisture sorption profile of silica gel.

4. Conclusions

Interfacing a Raman spectrometer to a moisture sorption balance enabled the simultaneous collection of gravimetric and spectroscopic information. The usefulness of this hyphenated technique was demonstrated for five model pharmaceutical compounds: sulfaguanidine, cromolyn sodium, amorphous sucrose, ranitidine HCl, and silica gel which had different modes of interaction with water. The spectroscopic data provided additional structural and chemical information and could be used to elucidate that underlying mechanism for changes in water content as a function of RH. Principal components analysis was found to be useful to process the Raman spectral data and to extract information about the water–solid interactions. Scores plots were utilized to determine the time frame for specific interactions or transformations while the loadings were used to interpret the changes observed in the Raman spectra.

Acknowledgements

The authors would like to thank VTI Corporation for assistance with modifying the equipment so that the Raman probe could be interfaced to the SGA-100.

References

[1] G. Zografi, Drug Dev. Ind. Pharm. 14 (1988) 1905–1926.
[2] G. Zografi, B. Hancock, Topics in Pharmaceutical Sciences 1993, in: D.J.A. Crommelin, K.K. Midha, T. Nagai (Eds.), Proceedings of International Congress on Pharmaceutical Sciences of F.I.P, 5–10 September 1993, Medpharm Sci. Pub, Tokyo, Japan, 1994, pp. 405–419.
[3] R.A. Lane, G. Buckton, Int. J. Pharm. 207 (2000) 49–56.
[4] K.L. Vora, G. Buckton, D. Clapham, Eur. J. Pharm. Sci. 22 (2004) 97–105.
[5] J. Rantanen, H. Wikstrom, R. Turner, L.S. Taylor, Anal. Chem. 77 (2005) 556–563.
[6] C.M. Deeley, R.A. Spragg, T.L. Threlfall, Spectrochim. Acta Part A: Mol. Biomol. Spectrosc. 47 (1991) 1217–1223.
[7] H. Wikstrom, P.J. Marsac, L.S. Taylor, J. Pharm. Sci. 94 (2005) 209–219.
[8] L.S. Taylor, G. Zografi, Pharm. Res. 15 (1998) 755–761.
[9] L.S. Taylor, F.W. Langkilde, J. Pharm. Sci. 89 (2000) 1342–1353.
[10] O. Svensson, M. Josefson, F.W. Langkilde, Eur. J. Pharm. Sci. 11 (2000) 141–155.
[11] R.J. Barnes, M.S. Dhanoa, S.J. Lister, Appl. Spectrosc. 43 (1989) 772–777.
[12] V. Andronis, M. Yoshioka, G. Zografi, J. Pharm. Sci. 86 (1997) 346–351.
[13] B. Makower, W.B. Dye, J. Agric. Food Chem. 4 (1956) 72–77.
[14] A.K. Salameh, L.S. Taylor, Pharm. Res. 22 (2005) 318–324.
[15] K. Uzunarslan, J. Akbuga, Pharmazie 46 (1991) 273–275.
[16] J.T. Carstensen, M.K. Franchini, Drug Dev. Ind. Pharm. 21 (1995) 523–536.
[17] J.S.G. Cox, G.D. Woodard, W.C. McCrone, J. Pharm. Sci. 60 (1971) 1458–1465.
[18] L.R. Chen, V.G. Young, D. Lechuga-Ballesteros, D.J.W. Grant, J. Pharm. Sci. 88 (1999) 1191–1200.